PNAS RESEARCH ARTICLE | PLANT BIOLOGY

Genetic robustness control of auxin output in priming organ initiation

Yuqiu Dai[a,1], Linjie Luo[b,c,1], and Zhong Zhao[a,2]

Edited by Elliot Meyerowitz, HHMI and California Institute of Technology, Pasadena, CA; received December 20, 2022; accepted May 17, 2023

Auxin signaling is essential for organ initiation in plants. How genetic robustness controls auxin output during organ initiation is largely unknown. Here, we identified *DORNROSCHEN-LIKE* (*DRNL*) as a target of MONOPTEROS (MP) that plays essential roles in organ initiation. We demonstrate that MP physically interacts with DRNL to inhibit cytokinin accumulation by directly activating *ARABIDOPSIS HISTIDINE PHOSPHOTRANSFER PROTEIN 6* and *CYTOKININ OXIDASE 6*. *DRN*, the paralogous gene of *DRNL*, acts redundantly with *DRNL* but is not coexpressed with *DRNL* in the organ founder cells in which *DRNL* is expressed. We demonstrate that DRNL directly inhibits *DRN* expression in the peripheral zone, whereas *DRN* transcripts are ectopically activated in *drnl* mutants and fully restore the functional deficiency of *drnl* in organ initiation. Our results provide a mechanistic framework for the robust control of auxin signaling in organ initiation through paralogous gene-triggered spatial gene compensation effects.

auxin | organ initiation | *DORNROSCHEN-LIKE* | spatial gene compensation | robustness control

Unlike animals, plants have the ability to develop new organs nearly throughout their entire lifespan. This ensures that sessile plants can survive various external pressures, such as environmental stresses, diseases, and predators. This vital ability depends on the activity of populations of stem cells in meristems, which have the capacity to self-renew as well as to give rise to daughter cells for lateral organ formation in both the shoot and root (1–4). The generation of the aboveground organs of higher plants depends on the maintenance and continuous differentiation of the shoot apical meristem (SAM), which is controlled by a complex regulatory network of signaling molecules (1, 3, 5, 6). Among these, phytohormones account for a large proportion, including auxin and cytokinin, which have been shown to be essential for SAM regulation (7–13). Cytokinin is enriched in the central zone (CZ), which harbors stem cells, and acts synergistically with auxin to maintain stem cell fate by activating *WUSCHEL* expression (8, 14, 15).

Auxin mainly accumulates in the differentiated peripheral zone (PZ), functioning in lateral organ initiation (7, 9, 16). The position and timing of organ initiation depends on the local accumulation of auxin maximum in the PZ by PINFORMED1 (PIN1)-mediated polar auxin transport (7, 16–19). Consistently, the loss-of-function mutants of *pin1* or *pinoid* (*pid*) fail to initiate organs during the reproductive stage (20, 21). In auxin signaling, AUXIN RESPONSE FACTOR5 (ARF5)/MONOPTEROS (MP) has been shown to be a key transcription factor that relays auxin signals during organ initiation, whose mutation also shows "pin-like" inflorescence as *pin1* and *pid* (8, 22). Given this critical role, multiple targets have been shown to be under direct control by MP during organ initiation, including *LEAFY* (*LFY*), *AINTEGUMENTA* (*ANT*), *ANT-LIKE6* (*AIL6*), *TARGET OF MONOPTEROS 3* (*TMO3*), and *FILAMENTOUS FLOWERS* (*FIL*) (10, 23). However, how MP-mediated auxin signaling robustly controls organ initiation remains poorly understood. Here, we identified *DORNROSCHEN-LIKE* (*DRNL*) as a direct target of MP in the PZ. DRNL interacts with MP and forms a complex mediating cytokinin–auxin cross talk during lateral organ initiation. We demonstrate that most known MP targets during organ initiation are also under direct control by DRNL. Although we observed functional redundancy between *DRNL* and its paralog *DORNROSCHEN* (*DRN*), *DRN* is not coexpressed with *DRNL* in organ founder cells. Surprisingly, we observed that *DRN* transcripts that were originally located in the CZ were ectopically activated in organ founder cells in the *drnl* mutant and fully restored the functional deficiency of *drnl* during organ initiation. We further demonstrate that *DRN* expression in the PZ is under direct negative control by DRNL and that DRNL-triggered spatial paralogous gene compensation mediates the robust control of auxin signaling during organ initiation.

Significance

In plants, MP (MONOPTEROS)-mediated auxin signaling is essential for organ initiation. We suggest a molecular framework for auxin in the robustness control of organ initiation in the meristem. We demonstrate that MP interacts with DRNL (DORNROSCHEN-LIKE) to trigger organ initiation by limiting cytokinin accumulation and activating *AINTEGUMENTA*, *AINTEGUMENTA-LIKE6*, *TARGET OF MONOPTEROS 3,* and *FILAMENTOUS FLOWERS* expression. Although *DRNL* and its paralog *DRN* are not coexpressed, they act redundantly during organ initiation. We show that in *drnl* mutants, *DRN* transcripts are ectopically activated in organ initiation sites to compensate for the functional deficiency of *drnl* in organ initiation. Our work suggests that a spatial gene compensation–based safety strategy in auxin signaling participates to the genetic robustness control of organ initiation.

Author contributions: Y.D., L.L., and Z.Z. designed research; Y.D. and L.L. performed research; Y.D., L.L., and Z.Z. analyzed data; and Y.D., L.L., and Z.Z. wrote the paper.

The authors declare no competing interest.

This article is a PNAS Direct Submission.

[1]Y.D. and L.L. contributed equally to this work.

[2]To whom correspondence may be addressed. Email: zhzhao@ustc.edu.cn.

This article contains supporting information online at https://www.pnas.org/lookup/suppl/doi:10.1073/pnas.2221606120/-/DCSupplemental.

Published July 3, 2023.

Results

***DRNL* Acts Downstream of Auxin in Lateral Organ Initiation.** *DRN* and its paralogous gene *DRNL* are previously shown to be involved in the regulation of the plant stem-cell pool under the direct control of auxin signaling (24). Interestingly, the mutation in *LEAFLESS* (*LFS*), the single ortholog of *DRN* and *DRNL* in tomato that can be induced by auxin, shows "pin-like" shoots (25). Consistently, in *Arabidopsis*, we observed that the *drn drnl* double mutant also showed severe defects in lateral organ initiation with 68% (153 out of 225) of the double mutant eventually forming a "pin-like" inflorescence (Fig. 1 *A*–*F* and *SI Appendix*, Fig. S1 *A*–*F*). We further quantified the silique numbers in the main inflorescence of double mutants and observed a significantly reduced number in the double mutant compared to either single mutants or wild-type plants (*SI Appendix*, Fig. S2), suggesting that *DRN* and *DRNL* act redundantly in controlling lateral organ initiation in the SAM. Conversely, overexpression of *DRNL* caused a large increase in the number of siliques (*SI Appendix*, Fig. S3). Although *DRN* is not expressed in the PZ where lateral organs are initiated in wild-type plants (24, 26, 27), we did find that *DRNL* was expressed in the outer PZ where organs were initiated (Fig. 1*N* and *SI Appendix*, Fig. S4), as previously shown (24, 26–29), which was further confirmed by *DRNL::3×GFP* transgenic plants (Fig. 1 *H* and *K*). Furthermore, we generated *DRNL::DRNL-GFP* transgenic plants with the upstream sequences of *DRNL* that were previously reported (30) and observed that DRNL proteins were specifically expressed during organ initiation (Fig. 1 *I* and *L*).

DRN, a paralogous gene of *DRNL*, has been shown to be under direct control of the key transcription factor ARF5/MP in auxin signaling (24, 31), and the *drn drnl* double mutant showed "pin-like" inflorescence phenocopying the weak allele of *mp-S319* (8) (Fig. 1*G* and *SI Appendix*, Fig. S1*G*). We therefore tested whether *DRNL* expression was regulated by MP-mediated auxin signaling. We crossed the *DRNL::3×GFP* transgenic plants with the *mp-S319* mutant and observed a dramatic decrease in *DRNL* expression in the *mp* mutant (Fig. 1 *H*, *K*, *J*, and *M*), which was further confirmed using in situ hybridization (Fig. 1 *N* and *O*) and quantitative reverse transcription PCR (qRT–PCR) on wild-type and *mp* mutant plants (Fig. 1*S*). This suggested that *DRNL* is under positive control by MP. Support for this idea came from the observation that the transcript and protein accumulation domains of *DRNL* overlapped with *MP* in the PZ during organ initiation (*SI Appendix*, Fig. S5), and two auxin response elements (AuxREs) have been shown to be necessary for *DRNL* expression in the SAM (28). Consistent with the early observation that *DRNL* is regulated by auxin (32), we observed that *DRNL* transcripts were significantly increased after treatment with indole-3-acetic acid (IAA) and naphthalene acetic acid (NAA) for 2 h (Fig. 1 *T* and *U*).

To determine whether endogenous auxin contributes to the regulation of *DRNL* expression, we analyzed the *yuc1 yuc2 yuc4 yuc6* quadruple mutant lacking essential auxin biosynthesis genes (33) and observed a dramatic decrease in *DRNL* transcripts in the quadruple mutant (Fig. 1 *N*, *R*, and *W*). Consistently, using the chemical treatment of yucasin to reduce the endogenous auxin levels by inhibiting the expression of *YUCCA* genes (34), we observed that the expression of *DRNL* decreased significantly (Fig. 1*V*). The local accumulation of auxin in the PZ is essential for new organ initiation, which is achieved by auxin polar transport. In *pinformed1* (*pin1*) and *pinoid* (*pid*) mutants with compromised auxin polar transport, we observed a dramatic decrease in *DRNL* expression (Fig. 1 *N*, *P*, *Q*, and *W*). To avoid effects on expression from morphological defects in *pin1* and *pid* that fail to initiate organs during the reproductive stage, we treated plants with the auxin transport inhibitor N-1-naphthylphthalamic acid (NPA). *DRNL* expression was decreased just 1 d after treatment and showed continued declines with increasing treatment time (*SI Appendix*, Fig. S6). Because the first visible phenotypes occurred only 5 d after treatment with NPA (8), we concluded that the reduction in *DRNL* transcripts was directly caused by the loss of local auxin accumulation in the SAM.

Given that *DRNL* expression was significantly elevated upon auxin treatment, we then tested whether *DRNL* expression in the SAM was under direct control by auxin response factors. To this end, we performed dexamethasone (DEX) induction on *RPS5A::GR-bdl* transgenic plants, in which mutated bdl (BODENLOS) proteins inactivated several ARFs, including MP, by direct binding, which cannot be degraded by intracellular auxin (35). We observed that *DRNL* expression drastically decreased upon DEX induction accompanied by treatment with the protein biosynthesis inhibitor cycloheximide (Fig. 1*X*). As *DRNL* expression was decreased in the *mp* mutant, *DRNL* is likely under direct positive control by MP. To test the interaction between *MP* and *DRNL* genetically, we expressed *DRNL* from the *p16* promoter (36) in *mp* mutants, whose promoter has been shown to be highly active in the SAM. Concomitant with a repression of *DRNL* in the *mp* mutant, we observed that overexpressed *DRNL* partially rescued the primordium initiation defects in *mp* mutants (Fig. 1 *Y* and *Z*), demonstrating that activation of *DRNL* transcription is a relevant aspect of MP functions in priming lateral organ initiation.

Cytokinin Signaling Was Disturbed in the *drn drnl* Mutant. A-type *ARABIDOPSIS RESPONSE REGULATORs* (*ARRs*) are primary response genes that can be rapidly induced by cytokinin (37). Previously, the expression of three *ARRs*, including *ARR4*, *ARR5*, and *ARR6*, was shown to be reduced in *35S::DRNL* transgenic plants (38). As *drn drnl* double mutants showed severe defects in organ initiation, it raises the possibility that *DRNL* was involved in the regulation of cytokinin signaling in the PZ that contributed to lateral organ formation. To test this hypothesis, we examined the activity of cytokinin signaling in the SAM by introducing the *two-component-output sensor* (*TCS*)*::dTomato* into *drn drnl* mutant plants. We observed extremely enlarged fluorescence signals of *TCS::dTomato* in almost the entire meristem of *drn drnl* plants (Fig. 2 *A*, *B*, *D*, and *E*), which was consistent with the early observation in tomato *lfs* mutants (25). This demonstrated that *DRNL*/*DRN* negatively regulates cytokinin signaling in the SAM. Given that *DRNL* was under direct positive control by MP-mediated auxin signaling (Fig. 1), we observed an even stronger accumulation of cytokinin in the SAM of *mp* mutants (Fig. 2 *A*, *C*, *D*, and *F*), suggesting that the *MP-DRNL*/*DRN* module mediates cytokinin–auxin cross talk during lateral organ initiation.

To shed light on the mechanism by which *DRNL* negatively regulates cytokinin, we examined the expression of cytokinin-related genes in biosynthesis, degradation and signal transduction in the SAM of the *drn drnl* mutant. Consistent with the increased cytokinin signaling, we observed that expression of the most cytokinin biosynthesis genes, including *ISOPENTENYL TRANSFERASEs* (*IPTs*) and *LONELY GUYs* (*LOGs*), was largely activated in *drn drnl* mutants (Fig. 2 *G* and *H*). Among the genes involved in cytokinin degradation, we observed that six of seven *CYTOKININ OXIDASE* (*CKX*) genes, except *CKX4*, were drastically reduced in the double mutant (Fig. 2*I*). Moreover, the inhibitor of cytokinin signaling *ARABIDOPSIS HISTIDINE PHOSPHOTRANSFER PROTEIN 6* (*AHP6*) was also observed to be repressed in *drn drnl* mutants (Fig. 2*J*). Similarly, the transcripts of most A-type *ARRs* that respond to cytokinin were significantly induced (*SI Appendix*, Fig. S7*A*).

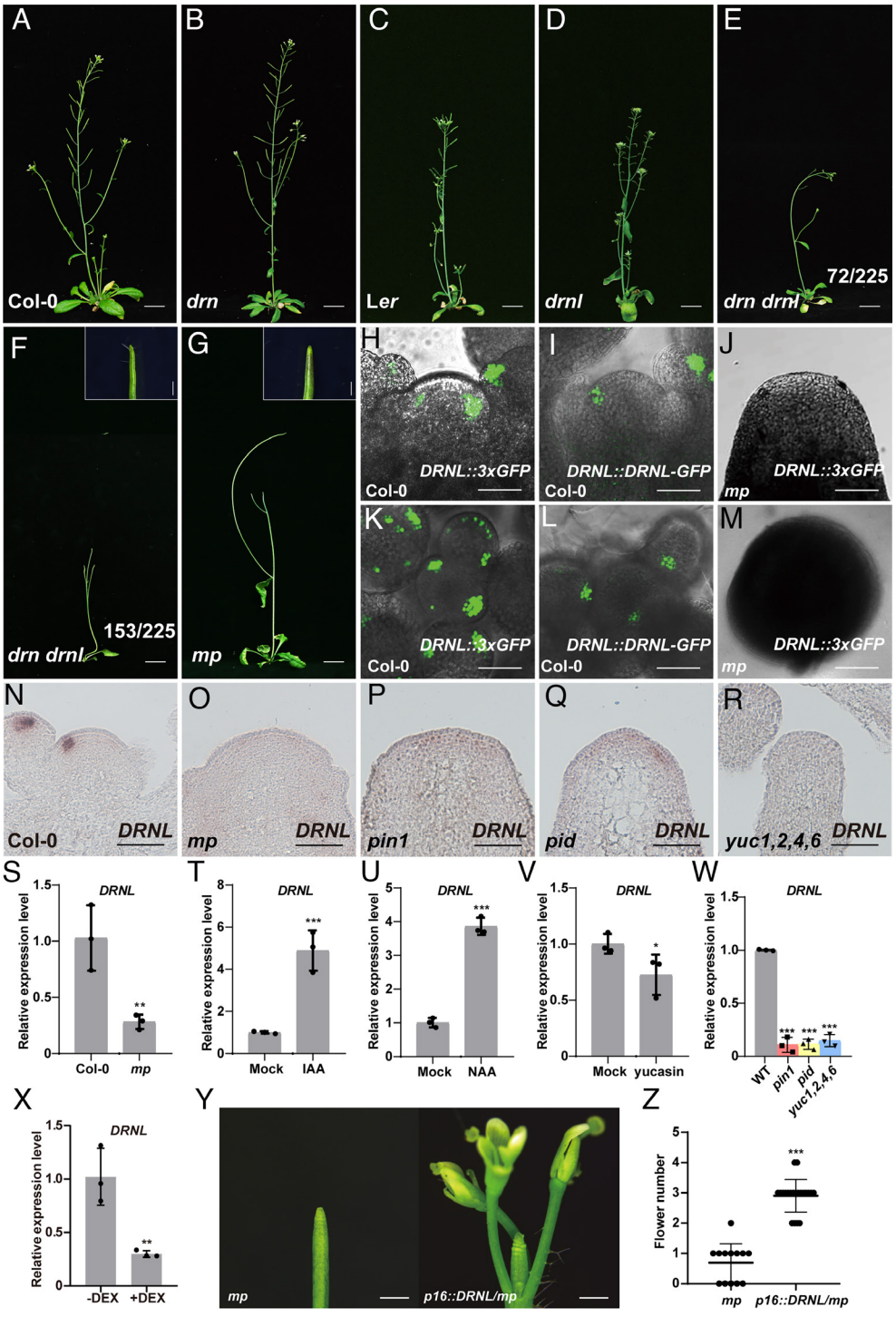

Fig. 1. *DRNL* acts downstream of auxin signaling in lateral organ initiation. (*A*–*G*) Six-week-old Col-0 (*A*), *drn* (*B*), L*er* (*C*), *drnl* (*D*), *mp* (*G*), and *drn drnl* (*E* and *F*) plants. The number of *drn drnl* mutants with different phenotypes is indicated (*E* and *F*). (Scale bars, 2 cm.) Magnification of the "pin-like" inflorescence of *drn drnl* (*F*) and *mp* (*G*) is shown in the upper right corner with scale bars 1 mm. (*H*–*M*) *DRNL* expression patterns in the SAM were detected by *DRNL::3×GFP* in Col-0 (*H* and *K*) and *mp* (*J* and *M*) plants. DRNL protein distribution patterns in *DRNL::DRNL-GFP* transgenic plants (*I* and *L*). (*K*–*M*) show the *Top* view of (*H*–*J*); n ≥ 10 shoot apexes per genotype were observed with similar results. (Scale bars, 50 μm.) (*N*–*R*) *DRNL* expression patterns in the SAM were detected by RNA in situ hybridization in Col-0 (*N*), *mp* (*O*), *pin1* (*P*), *pid* (*Q*) and *yuc1,2,4,6* (*R*) plants. n ≥ 12 shoot apexes per genotype were observed with similar results. (Scale bars, 50 μm.) (*S*–*W*) *DRNL* expression levels in the SAM of *mp* (*S*), *pin1pid* and *yuc1,2,4,6* (*W*) mutants, and IAA (*T*), NAA (*U*), yucasin (*V*) treatments measured by qRT–PCR. The data are shown as mean ± SD; n = 3 biological replicates, two-tailed Student's *t* tests, **P* < 0.05, ***P* < 0.01, ****P* < 0.001. (*X*) The expression levels of *DRNL* in the SAM of *RPS5A::GR-bdl* transgenic plants with or without DEX induction in the presence of cycloheximide. The data are shown as mean ± SD; n = 3 biological replicates, two-tailed Student's *t* tests, ***P* < 0.01. (*Y*) The "pin-like" inflorescence of *mp* is partially rescued by overexpressing *DRNL* under the *p16* promoter. (Scale bars, 1 mm.) (*Z*) Quantification of flower numbers of (*Y*). *mp* plants (n = 13); *p16::DRNL/mp* plants (n = 21), two-tailed Student's *t* tests, ****P* < 0.001.

DRNL Represses Cytokinin Signaling by Activating *AHP6* and *CKX6*. To identify the direct targets of *DRNL* in cytokinin signaling, we performed DEX induction on *UBQ10::DRNL-GR* transgenic plants combined with cycloheximide treatment. Among the genes that negatively regulate cytokinin accumulation and whose expression was reduced in the *drn drnl* mutant, we observed that the expression of *CKX6* and *AHP6* was significantly elevated upon DEX induction (Fig. 2 *K* and *L*). A-type *ARRs* (*SI Appendix*, Fig. S7*B*) and *LOGs* (*SI Appendix*, Fig. S8*B*) did not respond to induction. Although the expression levels of *IPT4*, *IPT6,* and *IPT8* were also reduced by DEX induction (*SI Appendix*, Fig. S8*A*), we failed to find any putative DRNL-binding site in their promoters. We therefore focused on *AHP6* and *CKX6*, two negative regulators of cytokinin. As shown in a previous study (39), we observed that *AHP6* was specifically expressed during organ initiation (Fig. 3*A*), and its expression pattern was similar to that of *DRNL* (Fig. 1*N*). Consistent with the notion that *AHP6* was activated by MP (39) and DRNL (Fig. 2*L*), *AHP6* transcripts were observed to be decreased in the *mp* (39), *drn drnl*, *pin1* and *pid* mutants (Fig. 3 *A*–*D*) but activated by IAA and NAA treatments (Fig. 3*E*). We further observed that the expression patterns of *CKX6* were similar to those of *DRNL* and *AHP6* (Fig. 3*H*), whose transcripts were also largely reduced in the *mp* (*SI Appendix*, Fig. S9), *drn drnl*, *pin1* and *pid* mutants (Fig. 3 *H*–*K*) but increased by auxin treatment (Fig. 3*L*). To further investigate whether DRNL could directly associate with

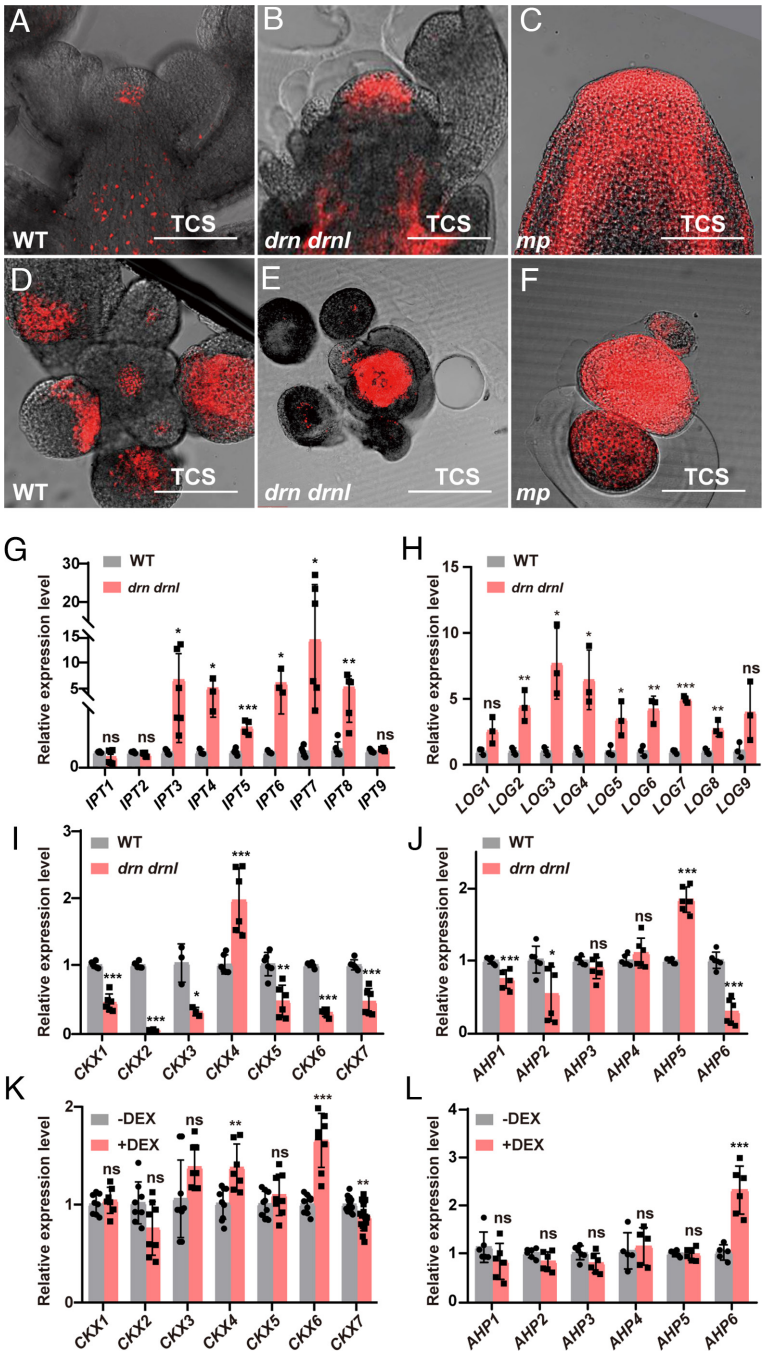

Fig. 2. Cytokinin signaling is disrupted in *drn drnl* and *mp* mutants. (*A*–*F*) Cytokinin signaling detected by *TCS::dTomato* in the inflorescence apexes of Col-0 (*A* and *D*), *drn drnl* (*B* and *E*), and *mp* (*C* and *F*) plants with longitudinal (*A*–*C*) and transverse sections (*D*–*F*). n ≥ 20 shoot apexes per genotype were observed with similar results. (Scale bars, 100 μm.) (*G*–*J*) Expression levels of cytokinin-related genes in biosynthesis, degradation, and signal transduction pathways in the SAM of the *drn drnl* mutant, including *IPTs* (*G*), *LOGs* (*H*), *CKXs* (*I*) and *AHPs* (*J*). The data are shown as mean ± SD; n ≥ 3 biological replicates, two-tailed Student's *t* tests, $*P < 0.05$, $**P < 0.01$, $***P < 0.001$; ns, no significant difference. (*K* and *L*) Expression levels of *CKXs* (*K*) and *AHPs* (*L*) in the inflorescence apexes of *UBQ10::DRNL-GR* plants with or without DEX induction in the presence of cycloheximide using qRT–PCR. The data are shown as mean ± SD; n ≥ 5 biological replicates, two-tailed Student's *t* tests, $**P < 0.01$, $***P < 0.001$; ns, no significant difference.

the *AHP6* and *CKX6* promoters, we performed ChIP assays with inflorescence apexes of *UBQ10::DRNL-GR* transgenic plants and observed the highest enrichment of DRNL in both the *AHP6* and *CKX6* promoters with fragments containing putative DRNL-binding sites of the GCC box (40) (Fig. 3 *F* and *M*). Moreover, using EMSAs, we demonstrated the direct binding of DRNL to exactly the ChIP-positive GCC box-containing fragments in the *AHP6* and *CKX6* promoters (Fig. 3 *G* and *N*). Thus, we concluded that DRNL directly activates *AHP6* and *CKX6* expression and mediates cytokinin–auxin cross talk during organ initiation.

To test this interaction genetically, we expressed *CKX6* and *AHP6* from the *MP* promoter in *drn drnl* mutants, which drives expression in the PZ. Concomitant with the decreases in *CKX6* and *AHP6* in the *drn drnl* mutant during organ initiation, we observed that the proportion of "pin-like" plants significantly decreased in both *MP::AHP6/drn drnl* and *MP::CKX6/drn drnl* transgenic plants compared with that of *drn drnl* mutants (*SI Appendix*, Fig. S10), suggesting that activation of *AHP6* or *CKX6* in the PZ partially rescued the primordia initiation defects in *drn drnl*.

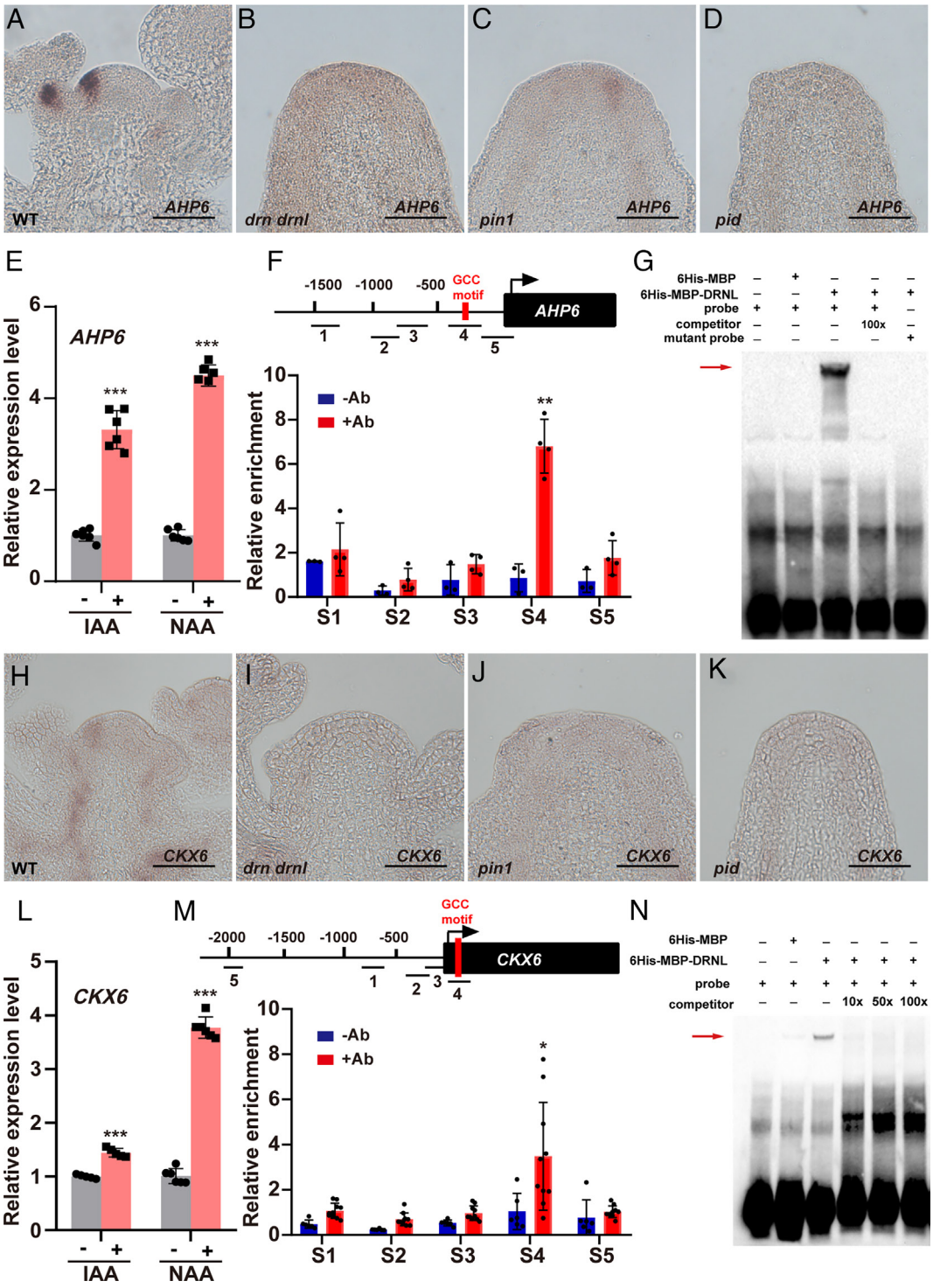

Fig. 3. DRNL directly activates *AHP6* and *CKX6* transcription in the shoot apical meristem. (*A–D*) *AHP6* expression patterns in WT (*A*), *drn drnl* (*B*), *pin1* (*C*), and *pid* (*D*) plants using RNA in situ hybridization; n ≥ 11 shoot apexes per genotype were observed with similar results. (Scale bars, 50 μm.) (*E*) Detection of *AHP6* expression levels in the SAM under IAA and NAA treatment using qRT–PCR. The data are shown as mean ± SD; n = 6 biological replicates, two-tailed Student's *t* tests, ***$P < 0.001$. (*F*) Enrichment of *AHP6* promoter fragments after ChIP using the inflorescence apexes of *UBQ10::DRNL-GR* plants; −Ab, no antibody control; +Ab, with GR antibody; red box, GCC motif; n = 4 biological replicates, two-tailed Student's *t* tests, **$P < 0.01$. (*G*) EMSA shows that DRNL specifically binds to the GCC motif of the *AHP6* promoter in vitro. The red arrow indicates the specific interactions. Two independent experiments were performed with similar results. (*H–K*) *CKX6* expression patterns in WT (*H*), *drn drnl* (*I*), *pin1* (*J*) and *pid* (*K*) plants using RNA in situ hybridization. n ≥ 8 shoot apexes per genotype were observed with similar results. (Scale bars, 50 μm.) (*L*) Detection of *CKX6* expression levels in the SAM under IAA and NAA treatment using qRT–PCR. The data are shown as mean ± SD; n = 5 biological replicates, two-tailed Student's *t* tests, ***$P < 0.001$. (*M*) Enrichment of *CKX6* promoter fragments after ChIP using the inflorescence apexes of *UBQ10::DRNL-GR* plants; −Ab, no antibody control; +Ab, with GR antibody; red box, GCC motif; n = 6 biological replicates, two-tailed Student's *t* tests, *$P < 0.05$. (*N*) EMSA shows that DRNL specifically binds to the GCC motif of the *CKX6* promoter in vitro. The red arrow indicates the specific interactions. Two independent experiments were performed with similar results.

MP and DRNL Form a Complex That Mediates Cytokinin–Auxin Cross Talk during Organ Initiation. Given that *AHP6* is under the direct control of both MP (39) and DRNL (Fig. 3 *F* and *G*), we then tested whether *CKX6* was also directly controlled by MP. To this end, we first examined *CKX6* expression in the *mp* mutant and observed a significant reduction similar to *AHP6* (39) (Fig. 4*A*). Using DEX induction on *RPS5A::GR-bdl* transgenic plants with cycloheximide treatment, we observed that both *CKX6* and *AHP6*

were repressed by the induction (Fig. 4*B*). We then tested whether MP could also associate with the *CKX6* promoter by performing ChIP assays with inflorescence apexes of *MP::MP-GFP/mp*-rescued plants. We observed significant enrichment of MP in three putative AuxREs in the *CKX6* promoter (Fig. 4*C*). By EMSAs, we mapped the binding of MP to the highest ChIP-positive AuxRE in the *CKX6* promoter (Fig. 4 *D–F*), suggesting that MP directly activates the expression of both *AHP6* and *CKX6*. Genetically, we expressed *CKX6* and *AHP6* in the *mp* mutant from the *MP* promoter and observed that the elevation of *AHP6* or *CKX6* partially rescued the organ initiation defects in *mp* mutants (Fig. 4 *G–L*). Our data demonstrate that *AHP6* and *CKX6*, at least in part, mediate auxin signaling in the PZ in priming organ initiation.

Because *AHP6* and *CKX6* were under direct positive control by both MP and DRNL, we hypothesized that these two transcription factors might form a complex to regulate the expression of *AHP6* and *CKX6*. To explore this possibility, we performed bimolecular fluorescence complementation (BiFC) experiments in tobacco leaves and observed an interaction between MP and DRNL in vivo (Fig. 4 *M–O*). To test their physical interaction in vitro, we conducted pull-down assays and observed that 6xHis-MBP-DRNL bound to GST-MP beads but not GST beads (Fig. 4*P*). Previously, *AIL6*, *ANT*, *FIL*, *LFY,* and *TMO3* were shown to be directly activated by MP during organ initiation (10, 23). We therefore tested whether these genes were also under direct control by DRNL. By performing DEX induction on *UBQ10::DRNL-GR* transgenic plants combined with cycloheximide treatment, we observed that four of five of these genes except *LFY* were significantly induced by DEX induction (*SI Appendix*, Fig. S11*A*). Our data demonstrate that MP activates the transcription of *DRNL* in the PZ and forms a complex to direct organ initiation by activating *AIL6*, *ANT*, *FIL,* and *TMO3* and repressing cytokinin accumulation in the PZ.

***DRNL*-Triggered Spatial Gene Compensation Mediates Auxin Signaling Robustness during Organ Initiation.** We have shown above that *DRN* and *DRNL* are functionally redundant in regulating organ initiation. However, the expression domains of *DRN* (Fig. 5*A*) and *DRNL* (Fig. 1*N*) in the SAM did not overlap in the wild-type plant (24, 26–28, 41). This was further confirmed using transgenic plants with both *DRN::mCherry* and *DRNL::3×GFP* reporters (Fig. 5 *E–H*). This raises a critical issue regarding how these two paralogs fulfill their redundancy in organ initiation. As *DRN* was not expressed in the organ founder cells in the wild type, we therefore examined *DRN* expression in the *drnl* mutant. To separate effects on expression from different genetic backgrounds, we generated a *drnl* #9 mutant using the CRISPR/Cas9 system (42) in the Col-0 background with only the first eight amino acids remaining correct (*SI Appendix*, Fig. S12). In contrast to the wild type, in which *DRN* is mainly expressed in the CZ (Fig. 5*A*), we observed an ectopic activation of *DRN* in the PZ where the lateral organ initiated in *drnl #9* mutant plants (Fig. 5*B*), which was further confirmed by the distribution of the *DRN* promoter reporter (Fig. 5 *C* and *D*) and DRN proteins (Fig. 5 *M–P* and *SI Appendix*, Fig. S13). To carry out a direct comparison, we crossed both *DRN::mCherry* and *DRNL::3×GFP* in the *drnl #9* mutant and observed colocalization of both genes in the primordia (Fig. 5 *I–L* and *SI Appendix*, Figs. S15 and S16), and the patterns were distinct from those in the wild-type plants (Fig. 5 *E–H* and *SI Appendix*, Figs. S14 and S16).

Consistent with the observation that *DRN* was activated ectopically in the organ founder cells in *drnl* mutants, we observed a significant increase in *DRN* transcripts in *drnl* mutant plants (Fig. 5*Q*). To examine whether DRNL directly repressed *DRN* at the transcriptional level, we performed DEX induction with cycloheximide on *UBQ10::DRNL-GR* plants and observed a significant reduction in *DRN* transcripts (Fig. 5*R*), suggesting that *DRN* is under direct negative control by DRNL. Thus, we tested whether DRNL associates with the *DRN* promoter by ChIP and found an interaction with fragments that contain the GCC element in the *DRN* promoter (Fig. 5*S*). Using EMSAs, we observed that DRNL bound to the ChIP-positive fragment specifically in vitro (Fig. 5*T*), indicating a direct role of DRNL in the negative regulation of *DRN* transcription.

If *DRN* was ectopically expressed in the *drnl* mutant and compensated for the functional deficiency of *DRNL* during organ initiation, we would expect that DRN should also directly activate *AHP6* and *CKX6* expression. Indeed, we observed that *AHP6* and *CKX6* expression levels were significantly increased upon DEX induction in *35S::DRN-GR* transgenic plants (*SI Appendix*, Fig. S17). Likely, the expression levels of *AIL6*, *ANT*, *FIL,* and *TMO3* were also increased in *35S::DRN-GR* transgenic plants upon induction (*SI Appendix*, Fig. S11*B*). Moreover, BiFC experiments in tobacco leaves (*SI Appendix*, Fig. S18*A*) and pull-down assays (*SI Appendix*, Fig. S18*B*) demonstrated that DRN can also directly interact with MP in plants. Our data demonstrate that *DRNL*-triggered spatial gene compensation is the molecular basis of the functional redundancy of *DRNL* and *DRN* in the PZ. This gene compensation–based safety strategy of *DRNL* participates in the genetic robustness of auxin signaling during organ initiation.

Our previous study showed that *DRN* expression was repressed by MP-mediated auxin signaling in the CZ (24). Given that MP proteins were highly accumulated in the PZ (*SI Appendix*, Fig. S5*B*), we then examined, in the *drnl* mutant background, whether ectopically expressed *DRN* in the PZ was activated or repressed by auxin signaling. Given that *DRN* did not affect its own expression (*SI Appendix*, Fig. S19*A*), we then examined *DRN* expression in *RPS5A::GR-bdl/drn drnl* plants with or without DEX induction. As the *drn-1* mutant contains a *dSpm* element insertion (41), we therefore designed primers upstream of the insertion site for qRT–PCR and subsequent in situ hybridization experiments. After DEX induction, we observed that *DRN* expression was significantly reduced using qRT–PCR and in situ hybridization (*SI Appendix*, Fig. S19 *B–D*), suggesting that ectopically expressed *DRN* in the *drnl* mutant was still activated by auxin signaling. MP and DRNL seem to be versatile transcriptional regulators that either activate or repress downstream genes in a tissue-specific manner or even in the same tissues. One possible mechanism underlying these effects could be that these versatile transcriptional regulators recruit different cofactors tissue specifically or target them specifically to direct the expression of downstream genes in opposite directions.

As *DRN* and *DRNL* also act redundantly in stem cells where *DRN* is expressed (24), we further tested whether *DRNL* also showed gene compensation effects in stem cells with *DRN*. Although *DRNL* expression levels were significantly increased in *drn* mutants (*SI Appendix*, Fig. S20*A*), we did not observe any direct effects of DRN in repressing *DRNL* expression in *35S::DRN-GR* plants (*SI Appendix*, Fig. S20*B*). Using in situ hybridization or reporter lines, we failed to detect any *DRNL* transcript, protein, or promoter activity in the CZ (*SI Appendix*, Fig. S20 *C–H*). A possible mechanism underlying these effects could be that the redundancy of *DRN* and *DRNL* in stem cells was indirectly mediated by an unknown mobile factor.

Discussion

Auxin and cytokinin play essential roles in the regulation of the SAM. In the CZ, which harbors undifferentiated stem cells, the functions of auxin and cytokinin are synergistic to maintain stem

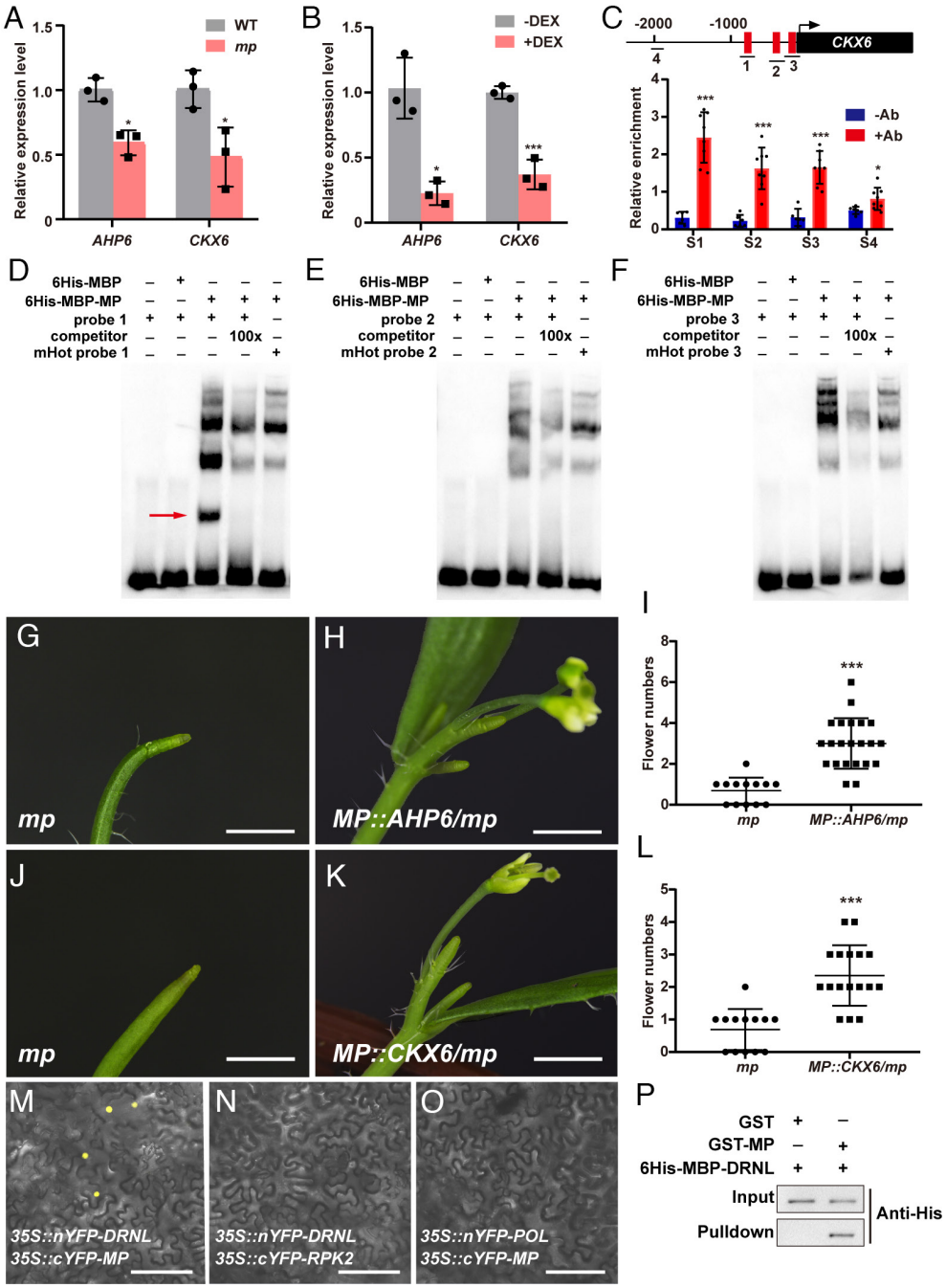

Fig. 4. The genetic interaction of the *MP-DRNL* module and *AHP6* and *CKX6* during organ initiation. (*A* and *B*) The expression levels of *AHP6* and *CKX6* in the SAM are decreased in *mp* (*A*) and *RPS5A::GR-bdl* plants with DEX and cycloheximide induction (*B*). The data are shown as mean ± SD; n = 3 biological replicates, two-tailed Student's *t* tests, **P* < 0.05, ****P* < 0.001. (*C*) Enrichment of *CKX6* promoter fragments after ChIP using the inflorescence apexes of *MP::MP-GFP/mp* plants; −Ab, no antibody control; +Ab, with GFP antibody, red box, AuxRE motif; n = 6 biological replicates, two-tailed Student's *t* tests, **P* < 0.05, ****P* < 0.001. (*D*–*F*) EMSA showing that MP binds to the first AuxRE motif of the *CKX6* promoter (*D*) in vitro. The red arrow indicates the specific interactions. Two independent experiments were performed with similar results. (*G*–*L*) The organ initiation defects in *mp* (*G* and *J*) were partially rescued in *MP::AHP6/mp* (*H* and *I*) and *MP::CKX6/mp* (*K* and *L*) plants, whose phenotypes were quantified by the numbers of flowers at 7 days after bolting (*I* and *L*). (Scale bars, 1 mm.) *mp* (*I*), n = 13; *MP::AHP6/mp*, n = 22; *mp* (*L*), n = 13; *MP::CKX6/mp*, n = 17; two-tailed Student's *t* tests, ****P* < 0.001. (*M*–*P*) MP interacts with DRNL in vivo in tobacco leaves by BiFC (*M*) and in vitro by pull-down assays (*P*). *35S::cYFP-RPK2* (*N*) and *35S::nYFP-POL* (*O*) were used as negative controls for BiFC, n ≥ 6 for each of three independent experiments. Two independent experiments were performed for pull-down assays (*P*) with similar results. (Scale bars, 50 μm.)

cell fate by activating *WUS* (8). Here, we showed that in the differentiated PZ, these two phytohormones are antagonistic in promoting lateral organ initiation. We demonstrated that *DRNL* is under positive control by MP-mediated auxin signaling. MP physically interacts with DRNL to inhibit cytokinin accumulation during organ initiation by directly activating *AHP6* and *CKX6*, whose genes are involved in both cytokinin signaling and degradation pathways to synergistically limit cytokinin levels in organ founder cells (Fig. 6). Consistently, *AHP6* (39) and *CKX6* (43) have also been shown to be induced by auxin in the regulation of phyllotaxis or developing leaf primordia under low red/far-red conditions. Because activation of *AHP6* or *CKX6* in the PZ could partially rescue the organ initiation defects in both *mp* and *drn drnl* mutants (Fig. 4 *G*–*L* and *SI Appendix*, Fig. S10), repression of cytokinin accumulation is a relevant aspect of MP function in the PZ. Support for this idea came from the

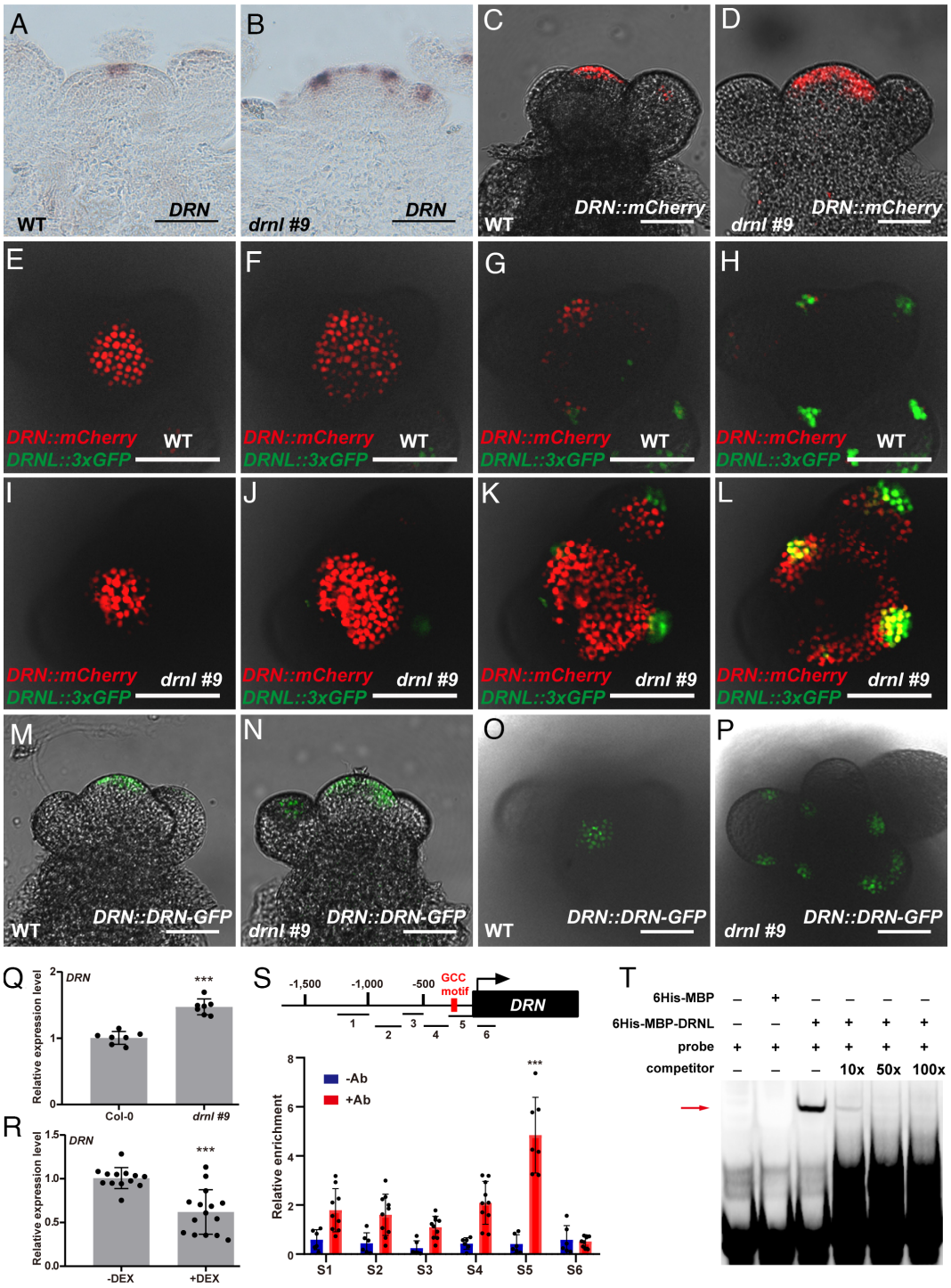

Fig. 5. *DRNL*-triggered spatial gene compensation mediated auxin signaling robustness during organ initiation. (*A–D*) *DRN* expression patterns in the SAM of WT Col-0 (*A* and *C*) and the *drnl* #9 mutant (*B* and *D*) detected by RNA in situ hybridization (*A* and *B*) and *DRN::mCherry* transgenic plants (*C* and *D*). n = 15 shoot apexes per genotype were observed with similar results (*A* and *B*); n ≥ 6 shoot apexes per genotype were observed with similar results (*C* and *D*). (Scale bars, 50 μm.) (*E–L*) *Top* view of *DRNL::3×GFP* and *DRN::mCherry* in WT Col-0 (*E–H*) and *drnl* #9 mutant (*I–L*) inflorescences in serial transverse sections imaged using an Olympus FV3000 confocal microscope. n ≥ 20 shoot apexes per genotype were observed with similar results (Scale bars, 50 μm.) (*M–P*) DRN protein distribution patterns in the inflorescences of *DRN::DRN-GFP* plants in the WT Col-0 (*M* and *O*) and *drnl* #9 (*N* and *P*) backgrounds; n ≥ 16 shoot apexes per genotype were observed with similar results. (Scale bars, 50 μm.) (*Q* and *R*) Detection of *DRN* expression levels in the SAM using the *drnl* #9 mutant (*Q*) and *UBQ10::DRNL-GR* plants with DEX and cycloheximide induction (*R*). The data are shown as mean ± SD; (*Q*), n = 7 biological replicates; (*R*), n ≥ 13 biological replicates; two-tailed Student's *t* tests, ***$P < 0.001$. (*S*) Enrichment of *DRN* promoter fragments after ChIP using the inflorescence apexes of *UBQ10::DRNL-GR* plants; −Ab, no antibody control; +Ab, with GR antibody; red box, GCC motif; n ≥ 6 biological replicates, two-tailed Student's *t* tests, ***$P < 0.001$. (*T*) EMSA shows that DRNL specifically binds to the *DRN* promoter in vitro. The red arrow indicates the specific interactions. Two independent experiments were performed with similar results.

observation that cytokinin is also overaccumulated in the "pin-like" shoot of *lfs* mutants in tomato (25). This suggests that DRNL/DRN-mediated cross talk between cytokinin and auxin is crucial for primordium initiation in the SAM. In addition to cytokinin, DRNL also directly activates the expression of *AIL6*, *ANT*, *FIL*, and *TMO3*, which are the known targets of MP in organ initiation, suggesting that MP-DRNL is a key module in auxin-mediated organ initiation.

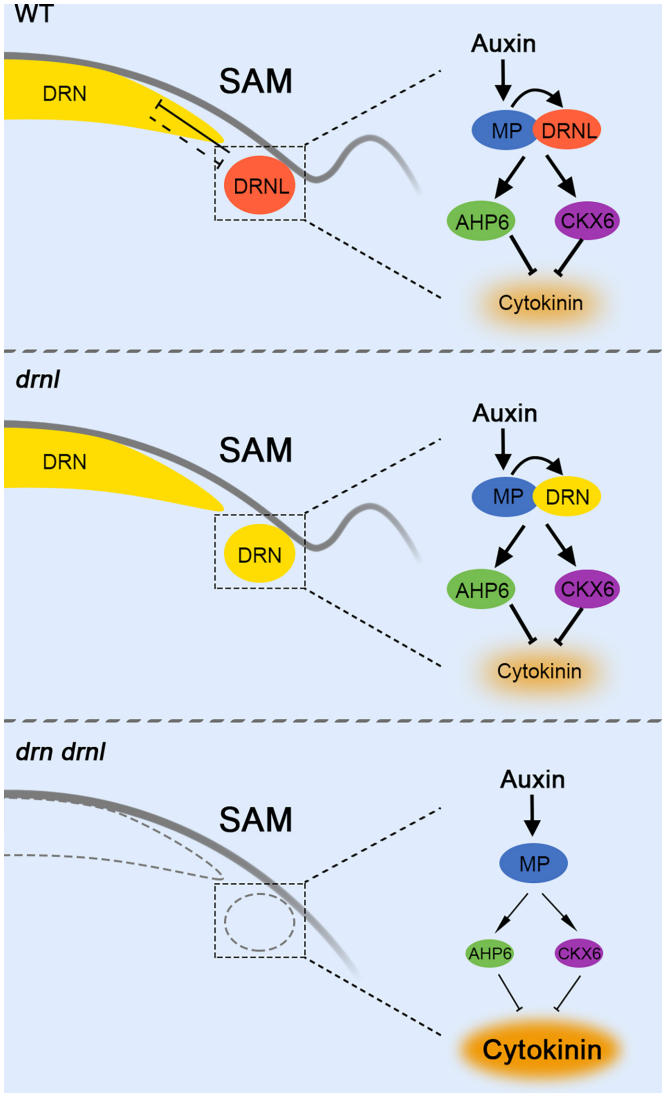

Fig. 6. Auxin-cytokinin cross talk during organ initiation mediated by *DRNL*-triggered spatial gene compensation. In the wild type, DRNL directly interacts with MP in the organ initiation cells in the PZ to inhibit cytokinin accumulation by activating *AHP6* and *CKX6*, which is essential for organ initiation. Although the expression and function of *DRN*, a paralog of *DRNL*, is mainly in the CZ, *DRN* transcripts are ectopically activated in the PZ in *drnl* mutants and fully restore the functional deficiency of *drnl* during organ initiation. In the *drn drnl* double mutant, cytokinin levels are highly accumulated resulting in severe defects in organ initiation. This spatial gene compensation triggered by DRNL provides a robust basis for auxin to promote organ initiation.

DRN and *DRNL* both belong to the largest subclass of the AP2/ERF gene family in *Arabidopsis* with only a single AP2 domain (44). These two paralogs are closely related with 91% similarity in the AP2 domain (*SI Appendix*, Fig. S21*A*) and act redundantly in embryonic development (45), shoot regeneration (30), floral development (27), axillary meristem formation (46), and stem cell maintenance (24). However, in the SAM, they show distinct spatial expression patterns, with *DRN* mainly in the CZ (Fig. 5*A*) and *DRNL* in the PZ (Fig. 1*N*). In this study, our data support a hypothesis of functional redundancy of the *DRN* and *DRNL* in regulating organ initiation. Although *DRN* was not expressed in the organ initiation site in the wild type, we demonstrate that *DRN* transcripts are ectopically activated in the *drnl* mutant to compensate for the loss of *DRNL* and restore the functional deficiency of *drnl* in organ initiation (Fig. 6). This gene compensation effect through spatial activation of the paralogous gene provides a molecular basis for auxin in the robustness control of organ initiation. Likely, in the rib zone of the SAM, the redundancy between CLAVATA1 (CLV1) and BARELY ANY MERISTEM (BAM) also relies on the ectopic expression of *BAM* genes to compensate for the loss of *CLV1* (47).

In the progress of evolution, how homologous genes generate and functionally diversify is a key question in understanding the origination of new genes and functions. During embryonic development, the expression of *DRN* is first observed in the two- to four-cell stage, while *DRNL* is expressed much later in the early globular embryo (41, 45, 48). Interestingly, from the globular stage to the heart stage, *DRN* and *DRNL* share similar expression patterns but diverge afterward (45, 48). We wondered whether this sequential expression difference of two paralogs in ontogeny might also reflect functional divergence during evolution. Support for this idea came from the observation that the origin of *DRN* was predicted to be 306 My while *DRNL* was 113 My by GenOrigin (http://genorigin.chenzxlab.cn/) (49) (*SI Appendix*, Fig. S21 *B* and *C*). A plausible scenario would then be that *DRNL* originated from a gene duplication event from the *DRN* and showed redundant functions in both stem cells and differentiated cells immediately following the duplication (*SI Appendix*, Fig. S22). During evolution, the functions of these two paralogous genes began to diverge. *DRN* expression is restricted in the CZ for stem cell maintenance by the direct repression of DRNL, whereas the function of *DRNL* is limited to differentiating cells indirectly by DRN (*SI Appendix*, Fig. S22). Despite their distinct expression patterns and biological functions, these two paralogs still show redundancy in both auxin-mediated stem cell maintenance and differentiation. The finding that *DRN* is directly repressed by DRNL in the PZ but ectopically reactivated in the *drnl* mutant fits well with the well-established "active compensation" model (50), which allows robust control of auxin during organ initiation.

Materials and Methods

Plant Materials and Growth Conditions. The *Arabidopsis thaliana* Columbia-0 (Col-0) ecotype was used except for *drnl* (*drnl-2, Ler* background). The seeds of *drn* (*drn-1*), *drnl* (*drnl-2*), *drn drnl* (*drn-1 drnl-2*), *mp-S319*, *RPS5A::GR-bdl*, *DRN::mCherry-N7*, *DRN::DRN-GFP*, *DRNL::3×GFP-N7* and *MP::MP-GFP*/*mp*-rescued plants have been described previously (24). The *TCS::dTomato* (51) transgenic plant was kindly provided by Yulin Jiao (Peking University). The *drnl* #9 mutant in the Col-0 background was generated by CRISPR/Cas9 (42). All transgenic plants were generated in the Col-0 ecotype. All seeds were sterilized by 70% ethanol and 0.5% Tween 20 for 10 min, followed by washing two times with 96% ethanol and air drying. Plants were grown on 1/2 Murashige and Skoog (MS) medium plates with 1% sucrose or on soil at 22 °C under long-day conditions (16 h light/8 h dark).

Chemical and Hormone Treatments. For DEX induction, inflorescence apexes were treated with 15 μM DEX and 50 μM cycloheximide in 1/2 MS liquid medium for 2 h. For hormone treatments, 1/2 MS liquid medium containing 50 μM IAA, 50 μM NAA, 50 μM NPA, or 100 μM yucasin was used for the treatment for 2 h supplied with 0.01% Silwet L-77, except where noted. For controls, 0.1% ethanol (mock) and 0.01% Silwet L-77 were used.

Plasmid Construction. For *DRNL::DRNL-GFP*, a 4.3-kb upstream sequence before the ATG of *DRNL* was used as a promoter according to a previous study (30). To generate DEX-inducible constructs, *DRNL* and *DRN* coding sequences (CDS) were subcloned downstream of the *UBQ10* and *35S* promoters to obtain *UBQ10::DRNL-GR* and *35S::DRN-GR*. To generate *p16::DRNL*, the *DRNL* coding sequence was subcloned downstream of a *p16* promoter, which is highly active in proliferating cells (36). For *MP::AHP6* and *MP::CKX6*, the full-length genomic sequences of *AHP6* and *CKX6* were cloned under the 4.1-kb promoter of *MP*. The primer sequences used in the plasmid construction are listed in *SI Appendix*, Table S1.

Total RNA Isolation and Quantitative RT–PCR. The inflorescence apexes of plants at 7 d after bolting were dissected as previously described and were immediately transferred to liquid nitrogen (52). Total RNA was isolated using TRI reagent (Sigma, T9424). The PrimeScript™ RT Reagent Kit (TaKaRa, RR047A) was used for cDNA synthesis. Quantitative PCR was performed using the ChamQ Universal SYBR qPCR Master Mix (Vazyme, Q711) in a Roche LightCycle 96 real-time PCR system with the following conditions: Step 1 to 95 °C for 5 min; Step 2 to 40 cycles of 95 °C for 10 s, followed by 57 °C for 30 s and 72 °C for 30 s; Step 3 to 72 °C for 10 min. The relative expression level of each gene was normalized to the housekeeping gene *TUBULIN*. The primer sequences used in qRT–PCR are listed in *SI Appendix*, Table S1.

Chromatin Immunoprecipitation (ChIP). ChIP was performed on the inflorescence apexes of *UBQ10::DRNL-GR* and *MP::MP-GFP*/*mp* plants, and 500-mg apexes were used for each independent experiment. ChIP was performed as previously described (8, 24) with minor modifications. A Diagenode Bioruptor UCD-200 was used for sonication (30 s on, 30 s off, medium, 15-min duration; sonication buffer: 10 mM Na_3PO_4, 100 mM NaCl, 10 mM EDTA, 0.5% sarkosyl, 1 mM PMSF, 1 tablet per 10 mL, pH 7). Anti-GR antibodies (Santa-sc-393232X) and anti-GFP antibodies (Abcam, ab290) were used to precipitate chromatin, and no antibody was used as a negative control. The bound DNA fragments were then analyzed using quantitative PCR. The primers used in the ChIP assays are listed in *SI Appendix*, Table S1.

Electrophoretic Mobility Shift Assay. The electrophoretic mobility shift assays (EMSAs) were performed as previously described (24, 53, 54). The CDS of *DRNL* and *MP* were cloned following a 6xHis-MBP tag to produce the recombinant proteins that were expressed in *Escherichia coli* strain Rosetta and purified with Nickel Sepharose™ 6 Fast Flow (GE Healthcare, 17-5318-01). The DNA probes were labeled with 5′-biotin, and unlabeled (cold) probes were used as specific competitors. A Light Shift Chemiluminescent EMSA kit (Thermo Scientific 20148) was used for the binding reactions. The primer sequences used in EMSAs are listed in *SI Appendix*, Table S1.

RNA In Situ Hybridization. RNA in situ hybridization was performed according to standard protocols as previously described (1, 55). The inflorescence apexes were harvested and fixed with FAA (50% ethanol, 5% acetic acid, 3.7% formaldehyde). After embedding in wax, sectioning was performed using Leica RM2235. Templates of RNA probes were amplified from cDNAs with gene-specific primers containing the T7 or T3 promoter sequence at the 5′ end. RNA probes were synthesized using T7/T3 polymerase and labeled with digoxin-UTP (Roche, 11277073910). The primer sequences are listed in *SI Appendix*, Table S1.

Confocal Microscopy. For the detection of fluorescence signals in the SAM, the inflorescence apexes were fixed and sectioned as previously described (24, 54). An Olympus FV3000 confocal microscope was used to obtain images in Fig. 5 and *SI Appendix*, Figs. S13–S16. The remaining confocal images were obtained using a Zeiss LSM710, except for *TCS::dTomato* signals, for which images were obtained using Olympus FV1200. To detect the GFP signals, a 488-nm laser was used for excitation, and a 500 to 550-nm emission spectrum was used for detection. mCherry was excited at 594 nm and detected at wavelengths between 590 and 632 nm. dTomato was excited at 554 nm and detected at wavelengths between 550 and 590 nm.

***Nicotiana Benthamiana* Infiltration.** *Agrobacterium tumefaciens* harboring relevant constructs was cultured at 28 °C for 2 d. The bacteria were then harvested by centrifugation at 3,500 rpm for 10 min and resuspended in infiltration buffer (10 mM MES, 10 mM $MgCl_2$, 150 μM acetosyringone, pH 5.8). The cells with different constructs were incubated for 2 h at room temperature and mixed with different combinations to infiltrate the abaxial surface of leaves in 3-wk-old *N. benthamiana* using an injector. Approximately 48 to 72 h after infiltration, the fluorescence signals were imaged with a Zeiss LSM710.

BiFC. For BiFC, *A. tumefaciens* containing plasmids of interest were transiently transformed into leaves of *N. benthamiana* and then detected using a Zeiss LSM710. The binary vectors *35S::nYFP-DRNL*, *35S::cYFP-MP,* and *35S::nYFP-DRN* were used to examine the protein–protein interaction, and *35S::nYFP-POL* and *35S::cYFP-RPK2* were used as negative controls.

Pull-Down Assays. Full-length *DRNL* CDS and the protein–protein interaction domain of *DRN* (residues 1 to 200) were cloned behind a 6xHis-MBP tag. The full-length *MP* CDS were cloned into the pGEX-6P-1 vector to generate the *GST-MP* construct. The 6xHis-MBP-fusion proteins were purified with Nickel Sepharose™ 6 Fast Flow (GE Healthcare, 17-5318-01). The GST and GST-MP proteins were purified with Glutathione Sepharose™ 4B (GE Healthcare, 17-0756-01), and beads were incubated with soluble 6xHis-MBP-fusion proteins at 4 °C overnight. The beads were washed six to eight times with a solution containing 20 mM Tris-HCl, pH 8.0; 200 mM NaCl; 1 mM EDTA, pH 8.0; 0.25% NP-40, and 25 ng/μL PMSF and then separated on an sodium dodecyl sulphate-polyacrylamide gel electrophoresis (SDS–PAGE gel) and immunoblotted using an anti-His antibody (Proteintech, 66005-1-Ig) at a 1:1,000 dilution.

Statistical Analysis. Differences between groups were identified using Student's *t* test, and the *P* value level was set at 5%.

Graph Drawing. Graphs with dot plots (individual data points) were drawn using GraphPad Prism 8.

Data, Materials, and Software Availability. All study data are included in the article and/or *SI Appendix*.

ACKNOWLEDGMENTS. We thank Prof. Yulin Jiao (Peking University) for sharing the *TCS::dTomato* transgenic plant. This work was supported by grants to Z.Z. from the National Natural Science Foundation of China (32130009, 31870264); University of Science and Technology of China Research Funds of the Double First-Class Initiative (YD9100002025); and the Strategic Priority Research Program of the Chinese Academy of Sciences (Grant No. XDB27030105).

Author affiliations: [a]Chinese Academy of Sciences Center for Excellence in Molecular Plant Sciences, Ministry of Education Key Laboratory for Cellular Dynamics, School of Life Sciences, Division of Life Sciences and Medicine, University of Science and Technology of China, Hefei 230027, China; [b]Anhui Provincial Key Laboratory of Molecular Enzymology and Mechanism of Major Diseases, College of Life Sciences, Anhui Normal University, Wuhu 241000, China; and [c]Anhui Provincial Key Laboratory of the Conservation and Exploitation of Biological Resources, College of Life Sciences, Anhui Normal University, Wuhu 241000, China

1. D. Weigel, G. Jurgens, Stem cells that make stems. *Nature* **415**, 751–754 (2002).
2. M. K. Barton, Twenty years on: The inner workings of the shoot apical meristem, a developmental dynamo. *Dev. Biol.* **341**, 95–113 (2010).
3. E. Aichinger, N. Kornet, T. Friedrich, T. Laux, Plant stem cell niches. *Annu. Rev. Plant Biol.* **63**, 615–636 (2012).
4. R. Heidstra, S. Sabatini, Plant and animal stem cells: Similar yet different. *Nat. Rev. Mol. Cell Biol.* **15**, 301–312 (2014).
5. B. Scheres, Stem cells: A plant biology perspective. *Cell* **122**, 499–504 (2005).
6. L. Williams, J. C. Fletcher, Stem cell regulation in the Arabidopsis shoot apical meristem. *Curr. Opin. Plant Biol.* **8**, 582–586 (2005).
7. D. Reinhardt *et al.*, Regulation of phyllotaxis by polar auxin transport. *Nature* **426**, 255–260 (2003).
8. Z. Zhao *et al.*, Hormonal control of the shoot stem-cell niche. *Nature* **465**, 1089–1092 (2010).
9. T. Vernoux *et al.*, The auxin signalling network translates dynamic input into robust patterning at the shoot apex. *Mol. Syst. Biol.* **7**, 508 (2011).
10. N. Yamaguchi *et al.*, A molecular framework for auxin-mediated initiation of flower primordia. *Dev. Cell* **24**, 271–282 (2013).
11. Z. J. Cheng *et al.*, Pattern of auxin and cytokinin responses for shoot meristem induction results from the regulation of cytokinin biosynthesis by AUXIN RESPONSE FACTOR3. *Plant Physiol.* **161**, 240–251 (2013).
12. G. E. Schaller, A. Bishopp, J. J. Kieber, The yin-yang of hormones: Cytokinin and auxin interactions in plant development. *Plant Cell* **27**, 44–63 (2015).
13. Z. H. Lee, T. Hirakawa, N. Yamaguchi, T. Ito, The roles of plant hormones and their interactions with regulatory genes in determining meristem activity. *Int. J. Mol. Sci.* **20**, 4065 (2019).
14. K. F. X. Mayer *et al.*, Role of WUSCHEL in regulating stem cell fate in the Arabidopsis shoot meristem. *Cell* **95**, 805–815 (1998).
15. S. P. Gordon, V. S. Chickarmane, C. Ohno, E. M. Meyerowitz, Multiple feedback loops through cytokinin signaling control stem cell number within the Arabidopsis shoot meristem. *Proc. Natl. Acad. Sci. U.S.A.* **106**, 16529–16534 (2009).
16. D. Reinhardt, T. Mandel, C. Kuhlemeier, Auxin regulates the initiation and radial position of plant lateral organs. *Plant Cell* **12**, 507–518 (2000).
17. E. Benkova *et al.*, Local, efflux-dependent auxin gradients as a common module for plant organ formation. *Cell* **115**, 591–602 (2003).
18. M. G. Heisler *et al.*, Patterns of auxin transport and gene expression during primordium development revealed by live imaging of the Arabidopsis inflorescence meristem. *Curr. Biol.* **15**, 1899–1911 (2005).
19. T. Vernoux, F. Besnard, J. Traas, Auxin at the shoot apical meristem. *Cold Spring Harb. Perspect. Biol.* **2**, a001487 (2010).
20. K. Okada, J. Ueda, M. K. Komaki, C. J. Bell, Y. Shimura, Requirement of the auxin polar transport system in early stages of Arabidopsis floral bud formation. *Plant Cell* **3**, 677–684 (1991).

21. S. R. M. Bennett, J. Alvarez, G. Bossinger, D. R. Smyth, Morphogenesis in pinoid mutants of Arabidopsis-thaliana. *Plant J.* **8**, 505–520 (1995).
22. G. K. H. Przemeck, J. Mattsson, C. S. Hardtke, Z. R. Sung, T. Berleth, Studies on the role of the Arabidopsis gene MONOPTEROS in vascular development and plant cell axialization. *Planta* **200**, 229–237 (1996).
23. M. F. Wu *et al.*, Auxin-regulated chromatin switch directs acquisition of flower primordium founder fate. *Elife* **4**, e09269 (2015).
24. L. J. Luo, J. Zeng, H. J. Wu, Z. X. Tian, Z. Zhao, A molecular framework for auxin-controlled homeostasis of shoot stem cells in Arabidopsis. *Mol. Plant* **11**, 899–913 (2018).
25. Y. Capua, Y. Eshed, Coordination of auxin-triggered leaf initiation by tomato LEAFLESS. *Proc. Natl. Acad. Sci. U.S.A.* **114**, 3246–3251 (2017).
26. J. W. Chandler, B. Jacobs, M. Cole, P. Comelli, W. Werr, DORNRA-SCHEN-LIKE expression marks Arabidopsis floral organ founder cells and precedes auxin response maxima. *Plant Mol. Biol.* **76**, 171–185 (2011).
27. J. W. Chandler, W. Werr, DORNROSCHEN, DORNROSCHEN-LIKE, and PUCHI redundantly control floral meristem identity and organ initiation in Arabidopsis. *J. Exp. Bot.* **68**, 3457–3472 (2017).
28. P. Comelli, D. Glowa, J. W. Chandler, W. Werr, Founder-cell-specific transcription of the DORNROSCHEN-LIKE promoter and integration of the auxin response. *J. Exp. Bot.* **67**, 143–155 (2016).
29. N. Prunet, W. B. Yang, P. Das, E. M. Meyerowitz, T. P. Jack, SUPERMAN prevents class B gene expression and promotes stem cell termination in the fourth whorl of Arabidopsis thaliana flowers. *Proc. Natl. Acad. Sci. U.S.A.* **114**, 7166–7171 (2017).
30. N. Matsuo, M. Makino, H. Banno, Arabidopsis ENHANCER OF SHOOT REGENERATION (ESR)1 and ESR2 regulate in vitro shoot regeneration and their expressions are differentially regulated. *Plant Sci.* **181**, 39–46 (2011).
31. M. Cole *et al.*, DORNROSCHEN is a direct target of the auxin response factor MONOPTEROS in the Arabidopsis embryo. *Development* **136**, 1643–1651 (2009).
32. H. Ram *et al.*, An integrated analysis of cell-type specific gene expression reveals genes regulated by REVOLUTA and KANADI1 in the Arabidopsis shoot apical meristem. *PLoS Genet.* **16**, e1008661 (2020).
33. Y. F. Cheng, X. H. Dai, Y. D. Zhao, Auxin synthesized by the YUCCA flavin Monooxygenases is essential for embryogenesis and leaf formation in Arabidopsis. *Plant Cell* **19**, 2430–2439 (2007).
34. T. Nishimura *et al.*, Yucasin is a potent inhibitor of YUCCA, a key enzyme in auxin biosynthesis (vol 77, pg 352, 2014). *Plant J.* **81**, 649–649 (2015).
35. D. Weijers *et al.*, Auxin triggers transient local signaling for cell specification in Arabidopsis embryogenesis. *Dev. Cell* **10**, 265–270 (2006).
36. C. Schuster *et al.*, A regulatory framework for shoot stem cell control integrating metabolic, transcriptional, and phytohormone signals. *Dev. Cell* **28**, 438–449 (2014).
37. J. P. C. To *et al.*, Type-A Arabidopsis response regulators are partially redundant negative regulators of cytokinin signaling. *Plant Cell* **16**, 658–671 (2004).
38. Y. Ikeda, H. Banno, Q. W. Niu, S. H. Howell, N. H. Chua, The ENHANCER OFSHOOT REGENERATION 2 gene in Arabidopsis regulates CUP-SHAPED COTYLEDON 1 at the transcriptional level and controls cotyledon development. *Plant Cell Physiol.* **47**, 1443–1456 (2006).
39. F. Besnard *et al.*, Cytokinin signalling inhibitory fields provide robustness to phyllotaxis. *Nature* **505**, 417–421 (2014).
40. H. Banno, H. Mase, K. Maekawa, Analysis of functional domains and binding sequences of Arabidopsis transcription factor ESR1. *Plant Biotechnol.* **23**, 303–308 (2006).
41. T. Kirch, R. Simon, M. Grunewald, W. Werr, The DORNROSCHEN/ENHANCER OF SHOOT REGENERATION1 gene of Arabidopsis acts in the control of meristem cell fate and lateral organ development. *Plant Cell* **15**, 694–705 (2003).
42. Z. P. Wang *et al.*, Egg cell-specific promoter-controlled CRISPR/Cas9 efficiently generates homozygous mutants for multiple target genes in Arabidopsis in a single generation. *Genome Biol.* **16**, 144 (2015).
43. M. Carabelli *et al.*, Canopy shade causes a rapid and transient arrest in leaf development through auxin-induced cytokinin oxidase activity. *Genes Dev.* **21**, 1863–1868 (2007).
44. J. M. Alonso *et al.*, Genome-wide insertional mutagenesis of Arabidopsis thaliana. *Science* **301**, 653–657 (2003).
45. J. W. Chandler, M. Cole, A. Flier, B. Grewe, W. Werr, The AP2 transcription factors DORNROSCHEN and DORNROSCHEN-LIKE redundantly control Arabidopsis embryo patterning via interaction with PHAVOLUTA. *Development* **134**, 1653–1662 (2007).
46. C. Zhang *et al.*, Spatiotemporal control of axillary meristem formation by interacting transcriptional regulators. *Development* **145**, dev158352 (2018).
47. Z. L. Nimchuk, Y. Zhou, P. T. Tarr, B. A. Peterson, E. M. Meyerowitz, Plant stem cell maintenance by transcriptional cross-regulation of related receptor kinases. *Development* **142**, 1043–1049 (2015).
48. J. W. Chandler, M. Cole, B. Jacobs, P. Comelli, W. Werr, Genetic integration of DORNROSCHEN and DORNROSCHEN-LIKE reveals hierarchical interactions in auxin signalling and patterning of the Arabidopsis apical embryo. *Plant Mol. Biol.* **75**, 223–236 (2011).
49. Y. B. Tong *et al.*, GenOrigin: A comprehensive protein-coding gene origination database on the evolutionary timescale of life. *J. Genet. Genomics* **48**, 1122–1129 (2021).
50. G. Diss, D. Ascencio, A. DeLuna, C. R. Landry, Molecular mechanisms of paralogous compensation and the robustness of cellular networks. *J. Exp. Zool. B Mol. Dev. Evol.* **322**, 488–499 (2014).
51. E. Zurcher *et al.*, A robust and sensitive synthetic sensor to monitor the transcriptional output of the cytokinin signaling network in planta. *Plant Physiol.* **161**, 1066–1075 (2013).
52. M. Schmid *et al.*, Dissection of floral induction pathways using global expression analysis. *Development* **130**, 6001–6012 (2003).
53. H. Wu *et al.*, WUSCHEL triggers innate antiviral immunity in plant stem cells. *Science* **370**, 227–231 (2020).
54. J. Zeng *et al.*, Endogenous stress-related signal directs shoot stem cell fate in Arabidopsis thaliana. *Nat. Plants* **7**, 1276–1287 (2021), 10.1038/s41477-021-00985-z.
55. S. U. Andersen *et al.*, Requirement of B2-type cyclin-dependent kinases for meristem integrity in Arabidopsis thaliana. *Plant Cell* **20**, 88–100 (2008).